

# Alteration of functional connectivity in patients with Alzheimer's disease revealed by resting-state functional magnetic resonance imaging

Jie Zhao<sup>1,2,3</sup>, Yu-Hang Du<sup>1</sup>, Xue-Tong Ding<sup>1</sup>, Xue-Hu Wang<sup>1,2,3,\*</sup>, Guo-Zun Men<sup>4</sup>

1 School of Electronic and Information Engineering, Hebei University, Baoding, Hebei Province, China

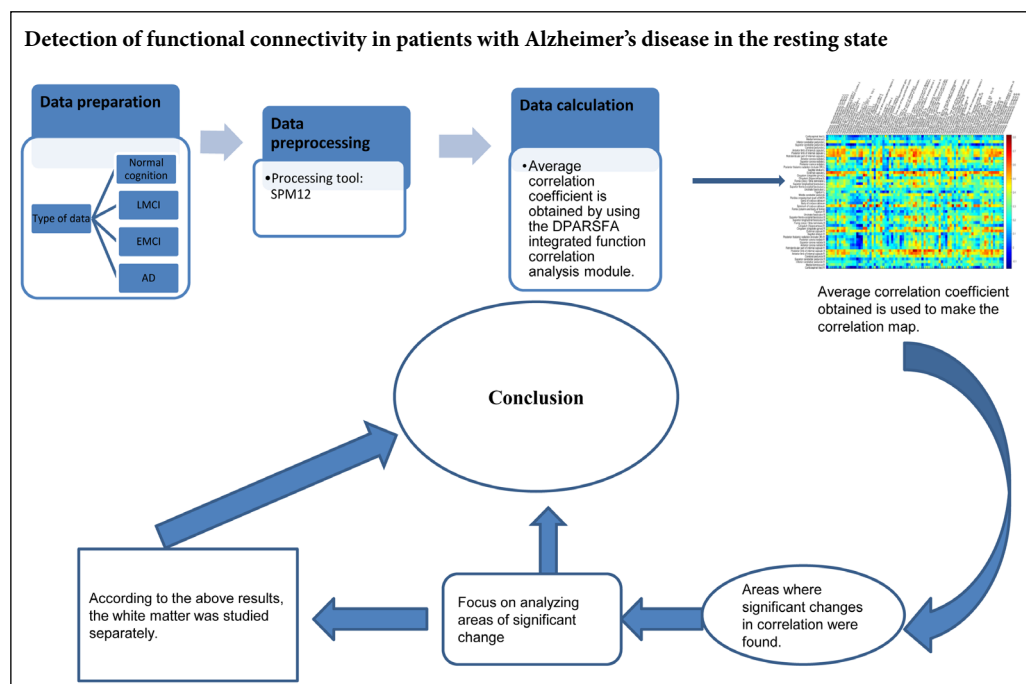
2 Research Center of Machine Vision Engineering & Technology of Hebei Province, Baoding, Hebei Province, China

3 Key Laboratory of Digital Medical Engineering of Hebei Province, Baoding, Hebei Province, China

4 School of Economics, Hebei University, Baoding, Hebei Province, China

**Funding:** This work was supported by the National Natural Science Foundation of China, No. 61401308, 61572063 (both to XHW); the Natural Science Foundation of Beijing of China, No. L172055 (to XHW); the Beijing Municipal Science & Technology Commission Research Fund of China, No. Z17110000417004 (to XHW); the China Postdoctoral Fund, No. 2018M631755 (to XHW); the Special Fund for Improving Comprehensive Strength of Hebei University in the Midwest of China, No. 801260201011 (to XHW); the High-Level Talent Funding Project — Selective Post-doctoral Research Project Fund of Hebei Province of China, No. B2018003002 (to XHW).

## Graphical Abstract



\*Correspondence to:

Xue-Hu Wang, PhD,  
wangxuehu\_tougao@163.com.

orcid:

0000-0001-9550-4073  
(Xue-Hu Wang)

doi: 10.4103/1673-5374.265566

Received: November 24, 2018

Accepted: June 26, 2019

## Abstract

The main symptom of patients with Alzheimer's disease is cognitive dysfunction. Alzheimer's disease is mainly diagnosed based on changes in brain structure. Functional connectivity reflects the synchrony of functional activities between non-adjacent brain regions, and changes in functional connectivity appear earlier than those in brain structure. In this study, we detected resting-state functional connectivity changes in patients with Alzheimer's disease to provide reference evidence for disease prediction. Functional magnetic resonance imaging data from patients with Alzheimer's disease were used to show whether particular white and gray matter areas had certain functional connectivity patterns and if these patterns changed with disease severity. In nine white and corresponding gray matter regions, correlations of normal cognition, early mild cognitive impairment, and late mild cognitive impairment with blood oxygen level-dependent signal time series were detected. Average correlation coefficient analysis indicated functional connectivity patterns between white and gray matter in the resting state of patients with Alzheimer's disease. Functional connectivity pattern variation correlated with disease severity, with some regions having relatively strong or weak correlations. We found that the correlation coefficients of five regions were 0.3–0.5 in patients with normal cognition and 0–0.2 in those developing Alzheimer's disease. Moreover, in the other four regions, the range increased to 0.45–0.7 with increasing cognitive impairment. In some white and gray matter areas, there were specific connectivity patterns. Changes in regional white and gray matter connectivity patterns may be used to predict Alzheimer's disease; however, detailed information on specific connectivity patterns is needed. All study data were obtained from the Alzheimer's Disease Neuroimaging Initiative Library of the Image and Data Archive Database.

**Key Words:** Alzheimer's disease; blood oxygen level-dependent signal; correlation coefficient; functional connectivity pattern; functional magnetic resonance imaging; gray matter; resting state; white matter

**Chinese Library Classification No.** R445; R447; R741

## Introduction

Alzheimer's disease (AD) is a progressive neurodegenerative disease with no obvious symptoms (Zhao et al., 2016; Koehler and Williams, 2018; Song et al., 2018). During AD onset, neurofibrillary tangles and amyloid  $\beta$ -peptide plaques in brain tissue can cause cortical dysfunction and damage (Nestor et al., 2004; Lin et al., 2018; Zhang et al., 2019). AD is characterized by memory loss, nerve atrophy, cell death, and diminished cognitive and language skills. AD reduces the ability to understand daily life, which causes certain behavioral disorders (Delbeuck et al., 2003; Karas et al., 2003). According to recent data, there were about 5.7 million patients with AD in the United States (US) in 2018, and this population is expected to reach 13.8 million in 2050 (Alzheimer's Association, 2018). ~1 million patients with dementia live in China, and the condition is conservatively estimated to cost approximately 60 billion US dollars each year (Chan et al., 2013; Xu et al., 2017). Moreover, AD prevalence is increasing worldwide, and, according to epidemiological data, over 135 million people may have AD in 2050 (Danborg et al., 2014). The disease progresses from onset to early mild cognitive impairment (EMCI), late mild cognitive impairment (LMCI), and, finally, AD, with the age of AD onset generally occurring around 65 years old.

AD pathogenesis can be studied using magnetic resonance imaging (MRI) to assess structural changes, functional MRI (fMRI) to measure functional activation patterns, and positron emission tomography to examine functional and metabolic changes with radiotracers. The most effective method is multi-modal neuroimaging; however, this is very expensive. In recent years, non-invasive and non-irradiating fMRI has been widely used as a leading technology in studies of mild cognitive impairment and AD. The fMRI method is a reliable tool for investigating functional connectivity, temporal and spatial correlations between different brain regions, and connectivity-based brain dysfunction (Ogawa et al., 1990). Low-frequency resting-state fMRI signal fluctuation is a major research area (Fox and Greicius, 2010) in which correlations between low-frequency fluctuations define brain functional connectivity (Biswal et al., 1995; Damoiseaux and Greicius, 2009). Furthermore, task-based fMRI is a relatively advanced technology that can be used to evaluate memory encoding (Machulda et al., 2003; Yetkin et al., 2006), vision (Rombouts et al., 2000), language (Kljajević, 2015), and auditory coding (Golden et al., 2015, 2016). Such studies provide evidence for specific functional connectivity patterns of task-associated brain regions and allow for the observation of disturbances or dysfunction within task-related areas subject to disease (Fleisher et al., 2009; Smitha et al., 2017). Compared with resting-state fMRI, task-based fMRI is very complicated and requires extensive subject coordination during data collection. In contrast, resting-state fMRI does not involve task performance. In addition, resting-state fMRI is very useful for identifying subtle differences in functional connectivity between diseases, which permits early disease detection and treatment development (Fox and Greicius, 2010).

AD research has gradually increased in recent years be-

cause of technological advancements, which have allowed researchers to identify diagnostic AD signs. Many AD researchers have reported gray matter atrophy in brain regions, including the temporal lobe and hippocampus (Frisoni et al., 2002; Karas et al., 2004). Other AD studies have found white matter volume reduction due to the loss of myelin and axons (Hua et al., 2008; Bartzokis, 2011; Braskie et al., 2012). In addition to its association with white and gray matter atrophy, AD may also be associated with regional brain connectivity. Functional connectivity anomalies can be detected before structural changes (Grady et al., 2001; Bozzali et al., 2002; Greicius et al., 2004; Jiang et al., 2004; Naggara et al., 2006; Stam et al., 2006; Wang et al., 2007; Bai et al., 2009; Kiuchi et al., 2009; Qi et al., 2010). In addition, some AD studies have reported blood oxygenation level changes in the sensorimotor cortex at rest (De Luca et al., 2005; Rosazza and Minati, 2011; Vahdat et al., 2011). Similar studies have also examined visual and auditory fMRI signal changes in AD (Cordes et al., 2000; Lowe et al., 2000; Schmidt et al., 2013; Golden et al., 2016). Liu et al. (2016) found that the intensity of hippocampal functional connectivity damage was associated with disease severity as subjects transitioned from EMCI to late-stage AD. Another study showed that poor episodic memory is associated with the anteroposterior dynamics of brain connections (Quevenco et al., 2017). Bero et al. (2012) demonstrated a bidirectional relationship between amyloid aggregation and reduced brain functional connectivity. Moreover, increases in functional connectivity were also found in other brain regions (Allen et al., 2007; Zhou et al., 2013).

At present, functional connectivity analysis, which statistically reflects the synchronicity of functional activities between non-adjacent brain regions (Arbabshirani et al., 2013), is the most commonly used resting-state fMRI analytical method. Recently, it has been shown that blood oxygen level-dependent (BOLD) signals can be detected in white matter, and it is suspected that the signals in white matter have the same properties as those in gray matter caused by neural activity (Ding et al., 2016). Ding et al. (2018) showed that white matter BOLD signals correlated with corresponding neural activity in the resting state, and that signal intensity was enhanced by functional stimulation. In addition, these authors analyzed specific connectivity patterns between white and gray matter during resting-state brain activity.

Considering the aforementioned studies, we propose that, in the resting state, patients with AD have specific connectivity patterns between certain white and gray matter regions, which can be used to predict AD based on connectivity pattern changes. In this study, a white and gray matter correlation map was obtained by processing resting-state BOLD signal data from patients with AD to assess regional changes in the white and gray matter. Furthermore, we performed a simple analysis of the white matter BOLD signal.

## Materials and Methods

### Data acquisition

All data were obtained from the Alzheimer's Disease Neu-

roimaging Initiative Library of the Image and Data Archive (<https://ida.loni.usc.edu/pages/access/search.jsp?>). In this library, imaging data from patients with mental retardation were collected and classified. Moreover, cognitive impairment data were collected from patients and classified as normal cognition, EMCI, LMCI, or AD. Database queries for specific data classification criteria were entered according to the following link: <http://adni.loni.usc.edu/data-samples/data-types/>. We downloaded normal cognition ( $n = 33$  patients), EMCI ( $n = 21$ ), LMCI ( $n = 21$ ), and AD ( $n = 39$ ) data acquired using a 3-T Philips Achieva scanner. The repetition time was 3 seconds; the matrix size was  $256 \times 256$ ; and the thickness of the slice was 3 mm. For anatomical reference, high resolution T1-weighted and BOLD signal images were acquired using a 3D multi-gradient echo sequence with a voxel size of  $1 \text{ mm}^3$ .

### Data processing

BOLD images were preprocessed using the statistical parametric mapping software package SPM12 ([www.fil.ion.ucl.ac.uk/spm/software](http://www.fil.ion.ucl.ac.uk/spm/software)). First, the images were corrected for slice timing and head motion, and subjects with large head motion ( $> 2 \text{ mm}$  in translation or  $> 2^\circ$  in rotation) were excluded. The corrected images were spatially smoothed with a  $4 \times 4 \times 4\text{-mm}^3$  full-width, half-maximum Gaussian kernel in each direction. Second, T1-weighted images were segmented into gray and white matter, and these images were registered to the mean motion-corrected BOLD image. Third, the smoothed BOLD and coregistered T1-weighted images as well as the gray and white matter segments were normalized to Montreal Neurological Institute space. Subsequent processing steps included BOLD image linear trend removal to correct for signal drifting and temporal low-pass filtering to retain frequencies below 0.1 Hz. Finally, in the preprocessed BOLD images, time points were normalized into unit variance voxelwise time series.

### Region of interest definition

Study analysis was limited to gray and white matter regions. The gray matter area mask was constructed according to Brodmann's atlas using the PickAtlas tool (Maldjian et al., 2003) and was used to divide the whole brain gray matter mask of each data set into 84 regions (42 per hemisphere). Simultaneously, a white matter tract mask was created using the JHU ICBM-DTI-81 WM Atlas (Mori et al., 2008). In each data set, these tract masks were applied to produce 48 tract regions (21 tracts and 3 combined tracts in each hemisphere). To accurately define a region of interest, the region of interest mask was selected from the stereotactic map of the fiber tract (Bürgel et al., 2006). The region of interest mask was manually edited to match the position and extent to those shown in Marussich et al. (2016). An adjusted region of interest mask replaced the original hypothalamic radiation mask (tract 12) from the JHU atlas. In addition, to avoid signal damage from nearby gray matter regions, all tract masks were limited to the whole brain white matter mask of each subject, with a threshold of 0.95. Finally, the

BOLD signal was averaged over each gray matter region and white matter tract to produce an average time series, which was then used to derive pairwise time correlations between gray and white matter structures.

### Data analysis

After preprocessing and region of interest placement, connectivity analysis of the BOLD signal was performed in SPM12. Functional connectivity refers to the temporal correlation of spontaneous BOLD activity in different brain regions. Thus, only a time correlation analysis of the BOLD signal is required. We analyzed the association between changes in white and gray matter functional connectivity and the degree of cognitive impairment.

First, processed BOLD signal data were averaged over the defined area to obtain an average time series. Second, an average time correlation matrix was generated. Then, a time-averaged correlation coefficient map (threshold correlation coefficients  $|\text{correlation coefficient}| > 0.4$ ) was plotted using the average correlation matrix. Third, under the  $|\text{correlation coefficient}| > 0.4$  condition, a paired  $t$ -test was performed. A significant  $P$  value  $< 0.05$  was obtained, indicating a significant correlation between functional connectivity changes and the degree of cognitive impairment. Finally, the temporal correlation between white and gray matter was established using average correlation coefficient map characteristics. From this information, we obtained a variation characteristic of the functional connectivity between the white and gray matter using the functional connectivity module integrating the DPARSF toolkit and SPM12. This analysis was performed by observing changes in correlation.

## Results

### Correlation between white and gray matter in patients with AD

In **Figure 1**, the abscissa displays 84 gray matter areas, whereas the ordinate displays 48 white matter regions. In this figure, colored horizontal stripes represent regions that are correlated in the resting state (**Figure 1A–D**). Each individual block represents the average correlation coefficient. As shown in **Figure 1**, the white and gray matter areas have correlated neural activity. Specifically, yellow-to-red blocks indicate a correlation between gray and white matter regions, with light yellow indicating a weak correlation ( $0.3 < 0.5$ ), dark yellow indicating a strong correlation ( $0.5\text{--}0.6$ ), and red indicating the most relevant regional correlation ( $> 0.6$ ). In the normal cognition group (**Figure 1A**), the white matter regions that were associated with gray matter were the medial lemniscus (ML), inferior cerebellar peduncle (ICBLP), superior cerebellar peduncle (SCBLP), cerebral peduncle (CBRP), anterior corona radiata (ACR), superior corona radiata (SCR), posterior corona radiata (PCR), retrolenticular part of the internal capsule (RLIC), sagittal stratum (SS), external capsule (EC), cingulum (cingulate gyrus; CGG), superior longitudinal fasciculus (SLF), genu of the corpus callosum (GCC), body of the corpus callosum (BCC), and splenium of the corpus callosum (SCC). The areas with

strong correlations were the ACR, SCR, PCR, EC, CGG, and SLF. Initially, we found that most of the correlations of the four map areas gradually weakened; however, some of them strengthened. **Figure 1B** shows the correlation between gray and white matter region BOLD signals in patients with EMCI. Compared with the normal cognition group, the EMCI group (**Figure 1B**) exhibited a small reduction in the yellow blocks, which indicated weakened or absent correlations between these regions. The correlations between the ML, ICBLP, SCBLP, CBRP, ALIC, PLIC, and RLIC (white matter) and primary somatosensory cortex, primary motor cortex, and somatosensory association cortex (gray matter) disappeared. There was minimal significant variation in the number of yellow blocks between the EMCI and LMCI (**Figure 1C**) groups. However, the number of lighter yellow blocks was higher in the LMCI group (**Figure 1B**), which suggests that these regional correlations decreased with increasing cognitive impairment and that regional functional connectivity changed. Comparison of the LMCI (**Figure 1C**) and AD (**Figure 1D**) groups showed correlations of the ML, ICBLP, SCBLP, CBRP. In the AD group, yellow blocks corresponding to gray matter areas disappeared, indicating that these areas were no longer relevant.

Concurrently, some areas showed strong correlations with AD progression. The correlations between the CGG, SLF, BCC, and SCC (white matter) and ventral posterior cingulate cortex and retrosubicular area (gray matter) were the strongest in patients with AD. These regional correlations gradually increased as the degree of cognitive impairment increased. In AD, the signal intensity of these four regions was enhanced, indicating that the function of these regions was affected, which led to changes in correlation.

#### Significant change in the correlation between white and gray matter

With our correlation map, we found a relationship between white matter tracts and gray matter areas. To further examine these relationships, five gray matter regions were selected, including the primary somatosensory cortex 1 (PSC1), primary somatosensory cortex 2 (PSC2), primary somatosensory cortex 3 (PSC3), primary motor cortex (PMC), and somatosensory association cortex (SAC). The correlation coefficients of nine white matter regions (*i.e.*, ML, ICBLP, SCBLP, CBRP, ALIC, PLIC, and RLIC) were determined. The coefficients for the different AD stages are listed in **Tables 1–5**.

**Table 1** shows the correlation coefficients between the nine white and five gray matter regions in the normal cognitive state, which is the control condition. **Tables 2 and 3** contain the correlation coefficients of the ML, ICBLP, SCBLP, CBRP, and RLIC, which correspond to the five gray matter regions in patients with cognitive impairment and AD. After examining the individual data, we found that the data in **Tables 1, 2, and 3** sequentially decreased, whereas the data in **Tables 1, 4, and 5** generally increased. When the range of changes from the overall data was examined, we found that the correlation coefficients between eight white matter regions (ML,

ICBLP, SCBLP, CBRP, RLIC, CGG, SLF, and SCC) and five gray matter regions were between 0.3–0.5 under normal conditions and that the correlation coefficients of the BCC were between –0.1–0.1. The coefficients in **Table 2** range from 0.2–0.4, and the coefficients in **Table 3** range from 0–0.2.

**Tables 4 and 5** show the correlation coefficients of the latter four white matter regions (CGG, SLF, BCC, and SCC) corresponding to the five gray matter regions (PSC1, PSC2, PSC3, PMC, and SAC) in the LMCI and AD patients. In **Table 4**, the coefficients of the CGG, SLF, and SCC are between 0.25–0.45, and those of the BCC are between 0.05–0.1. In **Table 5**, the coefficients are between 0.5–0.75. We found that the range of the ML, ICBLP, SCBLP, CBRP, and RLIC correlation coefficients gradually decreased as the degree of cognitive impairment increased. In patients with AD, the range decreased to 0–0.2. The correlation coefficient of the five gray matter regions with the CGG, SLF, BCC, and SCC increased. In patients with AD, the correlation coefficient range increased to 0.5–0.75, but the change was not significant. In this group, the BCC changed greatly. These findings are consistent with those from the correlation map analysis, which further indicates that there may be a white and gray matter connectivity pattern associated with AD progression and cognitive impairment.

#### Changes in white matter

We performed a separate study of the white matter using the original data. We used a single time-averaged BOLD signal from the white matter and generated a histogram of the time-averaged white matter BOLD signal during the four phases of AD progression (**Figure 2**).

In **Figure 2**, dark blue indicates the normal cognition group, red represents the EMCI group, green represents the LMCI group, and yellow represents the AD group. As the patients progressed to AD, the time-averaged BOLD signal showed a general weakening trend in the ML, ICBLP, SCBLP, CBRP, ALIC, PLIC, and RLIC. These regions show obvious regularity, which is consistent with the results for weakened regions shown in **Figure 1**. Specifically, changes in cognitive impairment may be associated with functional changes in these white matter regions.

#### Discussion

In patients with AD, we found that the correlation between white matter regions and some gray matter areas were significantly enhanced or weakened with worsening cognitive impairment. At rest, patients with AD showed a specific connectivity pattern in areas where white and gray matter correlations were enhanced or weakened. The connectivity of these regions changed during AD progression. This study provides support for the prediction of AD through connectivity change detection. Functional connectivity changes occur before structural changes, which allows for earlier AD prediction and solid treatment plan development. In addition, BOLD signals in the ML, ICBLP, SCBLP, CBRP, ALIC, PLIC, and RLIC showed the same results as those of the correlation change relationship. This suggests that the function

Zhao J, Du YH, Ding XT, Wang XH, Men GZ (2020) Alteration of functional connectivity in patients with Alzheimer's disease revealed by resting-state functional magnetic resonance imaging. *Neural Regen Res* 15(2):285-292. doi:10.4103/1673-5374.265566

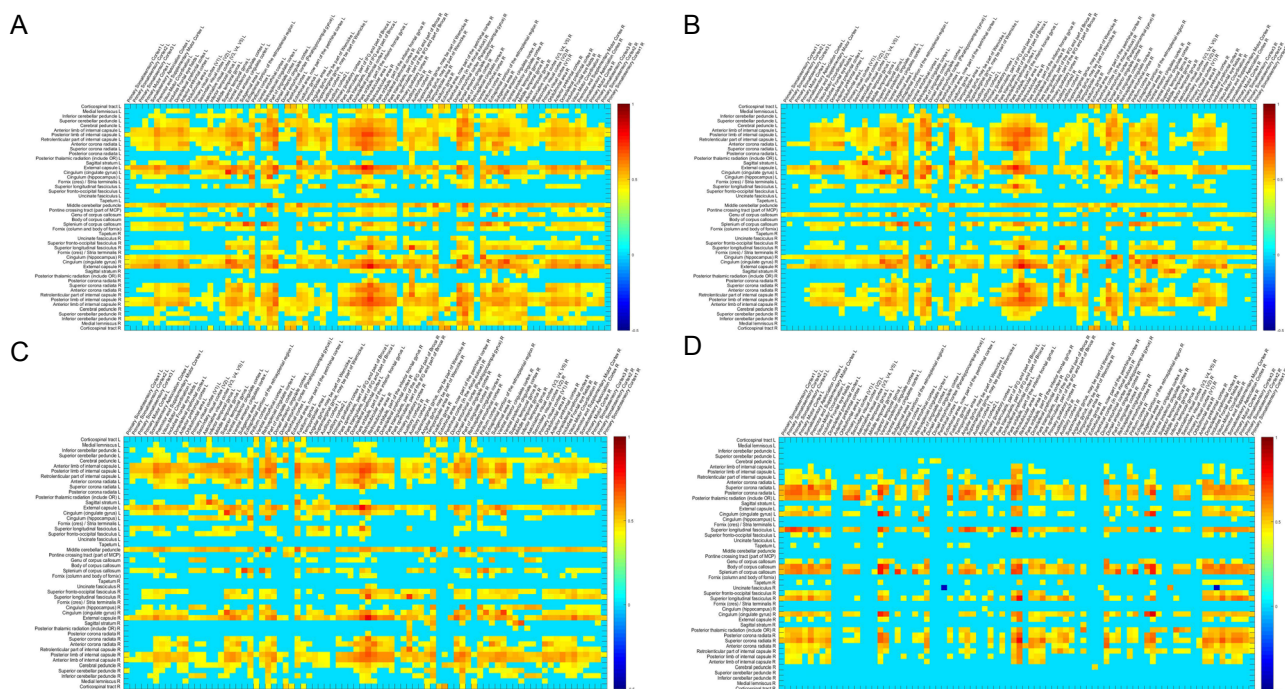


**Figure 1** Time-dependent images of the blood oxygen level-dependent signal in gray and white matter regions at rest. The colored blocks indicate the correlation between white and corresponding gray matter regions. The shade of the color indicates the strength of the correlation, with darker colors having stronger correlations. The colormap (right) indicates colors corresponding to the magnitude and direction (positive or negative) of the correlation. Threshold is at the mean  $|$ correlation coefficient $| > 0.4$ . (A–D) Normal cognition group (A), early mild cognitive impairment group (B), late mild cognitive impairment group (C), and Alzheimer's disease group (D).

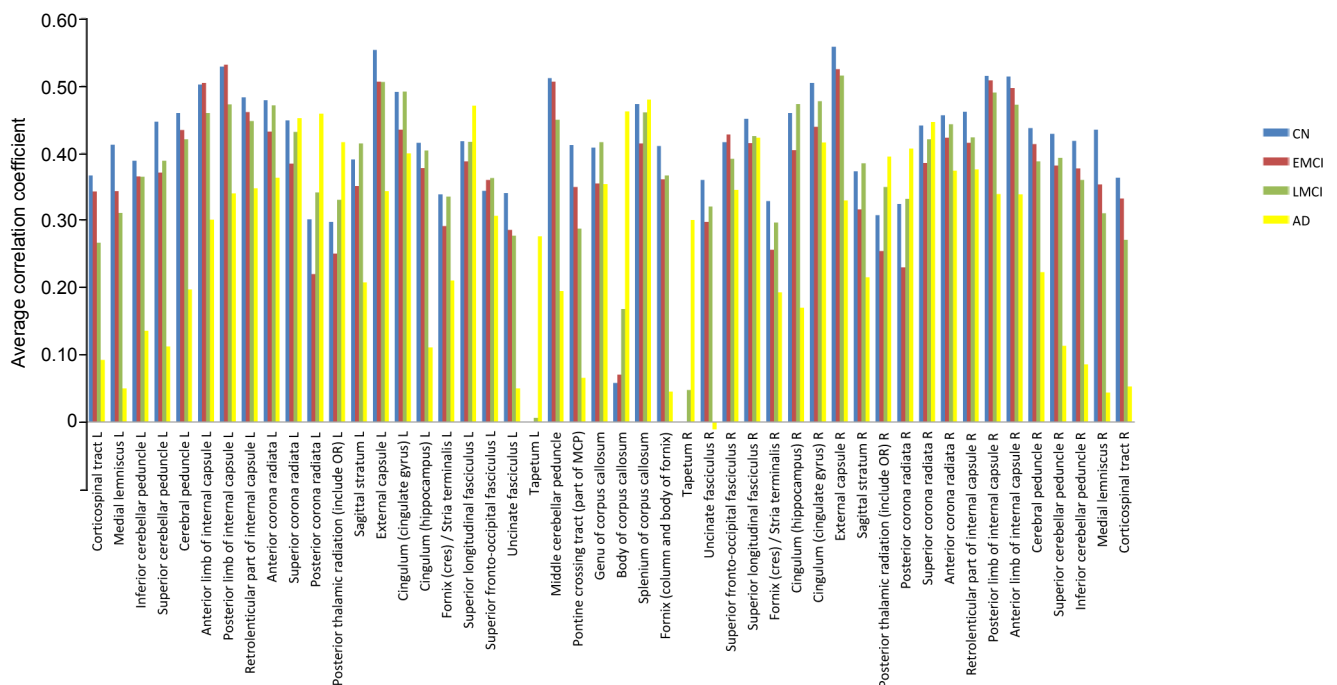


**Figure 2** Histogram of white matter correlation coefficients of patients with NC, EMCI, LMCI, and AD. The ordinate represents the average correlation coefficient. AD: Alzheimer's disease; EMCI: early mild cognitive impairment; L: left; LMCI: late mild cognitive impairment; NC: normal cognition; R: right.

Zhao J, Du YH, Ding XT, Wang XH, Men GZ (2020) Alteration of functional connectivity in patients with Alzheimer's disease revealed by resting-state functional magnetic resonance imaging. *Neural Regen Res* 15(2):285-292. doi:10.4103/1673-5374.265566

**Table 1 Correlation coefficient between white matter region and these five gray matter regions under normal cognition**

	PSC1	PSC2	PSC3	PMC	SAC
ML	0.33	0.33	0.34	0.38	0.35
ICBLP	0.33	0.4	0.37	0.37	0.41
SCBLP	0.35	0.36	0.35	0.41	0.38
CBRP	0.35	0.38	0.39	0.42	0.4
RLIC	0.35	0.43	0.44	0.44	0.46
CGG	0.38	0.45	0.48	0.49	0.48
SLF	0.34	0.4	0.42	0.42	0.41
BCC	0.05	-0.02	-0.02	0.03	-0.01
SCC	0.39	0.44	0.44	0.44	0.47

The table shows the average correlation coefficient under normal cognition. As reference control data. BCC: Body of corpus callosum; CBRP: cerebral peduncle; CGG: cingulum; ICBLP: inferior cerebellar peduncle; ML: medial lemniscus; PSC1: primary somatosensory cortex 1; PSC2: primary somatosensory cortex 2; PSC3: primary somatosensory cortex 3; PMC: primary motor cortex; RLIC: retrolenticular part of internal capsule; SAC: somatosensory association cortex; SCBLP: superior cerebellar peduncle; SCC: splenium of corpus callosum; SLF: superior longitudinal fasciculus.

**Table 2 Correlation parameters of white matter and gray matter regions in cognitive impairment**

	PSC1	PSC2	PSC3	PMC	SAC
ML	0.20*	0.21*	0.24*	0.26*	0.24*
ICBLP	0.22*	0.27*	0.26*	0.27*	0.27*
SCBLP	0.24*	0.30*	0.29*	0.31*	0.31*
CBRP	0.26*	0.33*	0.32*	0.31*	0.33*
RLIC	0.27*	0.36*	0.35*	0.33*	0.39*

The sign following the data in Table 2 indicates the relationship with the change of the corresponding data in Table 1. \* represents a decrease. CBRP: Cerebral peduncle; ICBLP: inferior cerebellar peduncle; ML: medial lemniscus; PMC: primary motor cortex; PSC1: primary somatosensory cortex 1; PSC2: primary somatosensory cortex 2; PSC3: primary somatosensory cortex 3; RLIC: retrolenticular part of internal capsule; SAC: somatosensory association cortex; SCBLP: superior cerebellar peduncle.

**Table 3 Correlation coefficient of these regions corresponding to Alzheimer's disease**

	PSC1	PSC2	PSC3	PMC	SAC
ML	0.07*	0.08*	0.07*	0.06*	0.02*
ICBLP	0.16*	0.16*	0.17*	0.18*	0.15*
SCBLP	0.10*	0.15*	0.12*	0.12*	0.11*
CBRP	0.15*	0.17*	0.20*	0.19*	0.14*
RLIC	0.37 <sup>#</sup>	0.44 <sup>#</sup>	0.45 <sup>#</sup>	0.46 <sup>#</sup>	0.41 <sup>#</sup>

The sign following the data in Table 3 indicates the relationship with the change of the corresponding data in Table 2. # indicates an increase with respect to the data in Table 2, \* represents a decrease. CBRP: Cerebral peduncle; ICBLP: inferior cerebellar peduncle; ML: medial lemniscus; PMC: primary motor cortex; PSC1: primary somatosensory cortex 1; PSC2: primary somatosensory cortex 2; PSC3: primary somatosensory cortex 3; RLIC: retrolenticular part of internal capsule; SAC: somatosensory association cortex; SCBLP: superior cerebellar peduncle.

**Table 4 Correlation coefficient between the following four white matter regions and gray matter in cognitive impairment**

	PSC1	PSC2	PSC3	PMC	SAC
CGG	0.31*	0.43 <sup>#</sup>	0.45*	0.42*	0.45*
SLF	0.27*	0.40 <sup>†</sup>	0.42 <sup>†</sup>	0.38*	0.39*
BCC	0.09 <sup>#</sup>	0.12 <sup>#</sup>	0.07 <sup>#</sup>	0.10 <sup>#</sup>	0.08 <sup>#</sup>
SCC	0.32*	0.41*	0.39*	0.38*	0.41*

The sign following the data in Table 4 indicates the relationship with the change of the corresponding data in Table 1. # indicates an increase with respect to the data in Table 1, \* represents a decrease, and † indicates no change. BCC: Body of corpus callosum; CGG: cingulum; PSC1: primary somatosensory cortex 1; PSC2: primary somatosensory cortex 2; PSC3: primary somatosensory cortex 3; PMC: primary motor cortex; SAC: somatosensory association cortex; SCC: splenium of corpus callosum; SLF: superior longitudinal fasciculus.

**Table 5 Correlation coefficient between four white matter regions and gray matter regions in Alzheimer's disease**

	PSC1	PSC2	PSC3	PMC	SAC
CGG	0.48 <sup>#</sup>	0.49 <sup>#</sup>	0.55 <sup>#</sup>	0.55 <sup>#</sup>	0.49 <sup>#</sup>
SLF	0.55 <sup>#</sup>	0.69 <sup>#</sup>	0.73 <sup>#</sup>	0.68 <sup>#</sup>	0.57 <sup>#</sup>
BCC	0.55 <sup>#</sup>	0.57 <sup>#</sup>	0.63 <sup>#</sup>	0.65 <sup>#</sup>	0.55 <sup>#</sup>
SCC	0.51 <sup>#</sup>	0.60 <sup>#</sup>	0.62 <sup>#</sup>	0.64 <sup>#</sup>	0.56 <sup>#</sup>

The sign following the data in Table 5 indicates the relationship with the change of the corresponding data in Table 4. # indicates an increase with respect to the data. BCC: Body of corpus callosum; CGG: cingulum; PSC1: primary somatosensory cortex 1; PSC2: primary somatosensory cortex 2; PSC3: primary somatosensory cortex 3; PMC: primary motor cortex; SAC: somatosensory association cortex; SCC: splenium of corpus callosum; SLF: superior longitudinal fasciculus.

of these white matter regions may be affected during AD progression, which lays a foundation for future white matter studies in patients with AD.

Future research should examine white matter to better predict AD. This study has certain limitations. Although there appears to be a certain connection mode, it was not clearly elucidated.

**Acknowledgments:** We are very grateful to Jing Liu, a lecturer of School of Electronic and Information Engineering, China, for her academic and constructive advices, and for correcting my paper. We are also very grateful to Fan Zhao and Xiao-Ying You, who offered the confidence and discussed with us about the paper.

**Author contributions:** Study concept and design: JZ, YHD, GZM; experimental implementation: YHD, XHW, XTD; data analysis: YHD; statistical analysis: YHD, XHW; paper writing: YHD. All authors approved the final version of the paper.

**Conflicts of interest:** The authors declare there are no conflicts of interest regarding the publication of this paper.

**Financial support:** This work was supported by the National Natural Science Foundation of China, No. 61401308, 61572063 (both to XHW); the National Science Foundation of Beijing of China, No. L172055 (to XHW); the Beijing Municipal Science & Technology Commission Research Fund of China, No. Z171100000417004 (to XHW); the China Postdoctoral Fund, No. 2018M631755 (to XHW); the Special Fund for Improving Comprehensive Strength of Hebei University in the Midwest of China, No. 801260201011 (to XHW); the China Postdoctoral Fund, No. 2018M631755 (to XHW); the High-Level Talent Funding Project — Selective Post-doctoral Research Project Fund of Hebei Province of China,

Zhao J, Du YH, Ding XT, Wang XH, Men GZ (2020) Alteration of functional connectivity in patients with Alzheimer's disease revealed by resting-state functional magnetic resonance imaging. *Neural Regen Res* 15(2):285-292. doi:10.4103/1673-5374.265566

No. B2018003002 (to XHW). The funding sources had no role in study conception and design, data analysis or interpretation, paper writing or deciding to submit this paper for publication.

**Institutional review board statement:** All data were obtained from Alzheimer's Disease Neuroimaging Initiative Library of The Image & Data Archive Database, which does not involve ethics and informed issues.

**Biostatistics statement:** The statistical methods of this study were reviewed by the biostatistician of Vanderbilt University.

**Copyright license agreement:** The Copyright License Agreement has been signed by all authors before publication.

**Data sharing statement:** This is an open access journal, and articles are distributed under the terms of the Creative Commons Attribution-Non-Commercial-ShareAlike 4.0 License, which allows others to remix, tweak, and build upon the work non-commercially, as long as appropriate credit is given and the new creations are licensed under the identical terms.

**Plagiarism check:** Checked twice by iThenticate.

**Peer review:** Externally peer reviewed.

**Open access statement:** This is an open access journal, and articles are distributed under the terms of the Creative Commons Attribution-Non-Commercial-ShareAlike 4.0 License, which allows others to remix, tweak, and build upon the work non-commercially, as long as appropriate credit is given and the new creations are licensed under the identical terms.

**Open peer reviewers:** Ivan Fernandez-Vega, Hospital Universitario Central de Asturias, Spain; Stavros I. Dimitriadis, Cardiff University Brain Research Imaging Centre (CUBRIC), UK; Paulina Carriba, Cardiff University, UK.

**Additional file:** Open peer review reports 1, 2 and 3.

## References

- Allen G, Barnard H, McColl R, Hester AL, Fields JA, Weiner MF, Ringe WK, Lipton AM, Brooker M, McDonald E, Rubin CD, Cullum CM (2007) Reduced hippocampal functional connectivity in Alzheimer disease. *Arch Neurol* 64:1482-1487.
- Alzheimer's Association (2018) 2018 Alzheimer's disease facts and figures. *Alzheimers Dement* 14:367-429.
- Arbabshirani MR, Havlicek M, Kiehl KA, Pearlson GD, Calhoun VD (2013) Functional network connectivity during rest and task conditions: a comparative study. *Human Brain Mapping* 34:2959.
- Bai F, Watson DR, Yu H, Shi Y, Yuan Y, Zhang Z (2009) Abnormal resting-state functional connectivity of posterior cingulate cortex in amnesic type mild cognitive impairment. *Brain Res* 1302:167-174.
- Bartzokis G (2011) Alzheimer's disease as homeostatic responses to age-related myelin breakdown. *Neurobiol Aging* 32: 1341-1371.
- Bero AW, Bauer AQ, Stewart FR, White, BR, Cirrito JR, Raichle ME, Culver JP, Holtzman DM (2012) Bidirectional relationship between functional connectivity and amyloid- $\beta$  deposition in mouse brain. *J Neurosci* 32:4334-4340.
- Biswal B, Zerrin Yetkin F, Haughton VM, Hyde JS (1995) Functional connectivity in the motor cortex of resting human brain using echo-planar MRI. *Magn Reson Med* 34:537-541.
- Bozzali M, Falini A, Franceschi M, Cercignani M, Zuffi M, Scotti G, Comi G, Filippi M (2002) White matter damage in Alzheimer's disease assessed in vivo using diffusion tensor magnetic resonance imaging. *J Neurol Neurosurg Psychiatry* 72:742-746.
- Braskie MN, Jahanshad N, Stein JL, Barysheva M, Johnson K, McMahon KL, de Zubicaray GI, Martin NG, Wright MJ, Ringman JM, Toga AW, Thompson PM (2012) Relationship of a variant in the NTRK1 gene to white matter microstructure in young adults. *J Neurosci* 32:5964-5972.
- Bürgel U, Amunts K, Hoemke L, Mohlberg H, Gilsbach JM, Zilles K (2006) White matter fiber tracts of the human brain: Threedimensional mapping at microscopic resolution, topography and intersubject variability. *Neuroimage* 29:1092-1105.
- Chan KY, Wang W, Wu JJ (2013) Epidemiology of Alzheimer's disease and other forms of dementia in China 1990-2010: a systematic review and analysis. *Lancet* 381:2016-2023.
- Cordes D, Haughton VM, Arfanakis K, Wendt GJ, Turski PA, Moritz CH, Quigley MA, Meyerand ME (2000) Mapping functionally related regions of brain with functional connectivity MR imaging. *Am J Neuroradiol* 21:1636-1644.
- Damoiseaux JS, Greicius MD (2009) Greater than the sum of its parts: a review of studies combining structural connectivity and resting-state functional connectivity. *Brain Struct Funct* 213:525-533.
- Danborg PB, Simonsen AH, Waldemar G (2014) The potential of microRNAs as biofluid markers of neurodegenerative diseases-a systematic review. *Biomarkers* 19:259-268.
- De Luca M, Smith S, De Stefano N, Federico A, Matthews PM (2005) Blood oxygenation level dependent contrast resting state networks are relevant to functional activity in the neocortical sensorimotor system. *Exp Brain Res* 167:587-594.
- Delbeuck X, Van der Linden M, Collette F (2003) Alzheimer's disease as a disconnection syndrome? *Neuropsychol Rev* 13:79-92.
- Ding Z, Huang Y, Bailey SK (2018) Detection of synchronous brain activity in white matter tracts at rest and under functional loading. *Proc Natl Acad Sci U S A* 115:595-600.
- Ding Z, Xu R, Bailey SK (2016) Visualizing functional pathways in the human brain using correlation tensors and magnetic resonance imaging. *Magn Reson Imaging* 34:8.
- Fleisher AS, Sherzai A, Taylor C, Langbaum JB, Chen K, Buxton RB, (2009) Resting-state BOLD networks versus task-associated functional MRI for distinguishing Alzheimer's disease risk groups. *Neuroimage* 47:1678-1690.
- Fox MD, Greicius M (2010) Clinical applications of resting state functional connectivity. *Front Syst Neurosci* 4:19.
- Frisoni G, Testa C, Zorzan A, Sabatelli F, Beltramello A, Soininen H, Laakso M (2002) Detection of grey matter loss in mild Alzheimer's disease with voxel based morphometry. *J Neurol Neurosurg Psychiatry* 73:657-664.
- Golden HL, Agustus JL, Goll JC, Downey LE, Mummery CJ, Schott JM, Crutch SJ, Warren JD (2015) Functional neuroanatomy of auditory scene analysis in Alzheimer's disease. *Neuroimage* 7:699-708.
- Golden HL, Agustus JL, Nicholas JM, Schott JM, Crutch SJ, Mancini L, Warren JD (2016) Functional neuroanatomy of spatial sound processing in Alzheimer's disease. *Neurobiol Aging* 39:154-164.
- Grady CL, Furey ML, Pietrini P, Horwitz B, Rapoport SI (2001) Altered brain functional connectivity and impaired short-term memory in Alzheimer's disease. *Brain* 124:739-756.
- Greicius MD, Srivastava G, Reiss AL, Menon V (2004) Default-mode network activity distinguishes Alzheimer's disease from healthy aging: evidence from functional MRI. *Proc Natl Acad Sci U S A* 101:4637-4642.
- Grodd W, Beckmann CF (2014) Resting state functional MRI of the brain. *Der Nervenarzt* 85:690.
- Hardy J, Selkoe DJ (2002) The amyloid hypothesis of Alzheimer's disease: progress and problems on the road to therapeutics. *Science* 297:353-356.
- Hua X, Leow AD, Parikshak N, Lee S, Chiang M-C, Toga AW, Jack CR, Weiner MW, Thompson PM, Alzheimer's Disease Neuroimaging Initiative (2008) Tensor-based morphometry as a neuroimaging biomarker for Alzheimer's disease: an MRI study of 676 AD, MCI, and normal subjects. *Neuroimage* 43:458-469.
- Jiang T, He Y, Zang Y, Weng X (2004) Modulation of functional connectivity during the resting state and the motor task. *Human Brain Mapp* 22:63-71.

Zhao J, Du YH, Ding XT, Wang XH, Men GZ (2020) Alteration of functional connectivity in patients with Alzheimer's disease revealed by resting-state functional magnetic resonance imaging. *Neural Regen Res* 15(2):285-292. doi:10.4103/1673-5374.265566

- Karas G, Scheltens P, Rombouts S, Visser P, Van Schijndel R, Fox N, Barkhof F (2004) Global and local gray matter loss in mild cognitive impairment and Alzheimer's disease. *Neuroimage* 23:708-716.
- Karas GB, Burton EJ, Rombouts SA, van Schijndel RA, O'Brien JT, h Scheltens P, McKeith IG, Williams D, Ballard C, Barkhof F (2003) A comprehensive study of gray matter loss in patients with Alzheimer's disease using optimized voxel-based morphometry. *Neuroimage* 18: 895-907.
- Kiuchi K, Morikawa M, Taoka T, Nagashima T, Yamauchi T, Makinodan M, Norimoto K, Hashimoto K, Kosaka J, Inoue Y (2009) Abnormalities of the uncinate fasciculus and posterior cingulate fasciculus in mild cognitive impairment and early Alzheimer's disease: a diffusion tensor tractography study. *Brain Res* 1287:184-191.
- Kljajević V (2015) Verbal fluency and intrinsic brain activity in Alzheimer's disease. *Croat Med J* 56:573.
- Koehler D, Williams FE (2018) Utilizing zebrafish and okadaic acid to study Alzheimer's disease. *Neural Regen Res* 13:1538-1541.
- Lin W, Yang LK, Zhu J, Wang YH, Dong JR, Chen T, Wang D, Xu XM, Sun SB, Zhang L (2018) Deep brain stimulation for the treatment of moderate-to-severe Alzheimer's disease: Study protocol for a prospective self-controlled trial. *Clin Trials Degener Dis* 3:66-70.
- Liu J, Zhang X, Yu C, Duan Y, Zhuo J, Cui Y, Liu B, Li K, Jiang T, Liu Y (2016) Impaired parahippocampus connectivity in mild cognitive impairment and Alzheimer's disease. *J Alzheimers Dis* 49:1051-1064.
- Lowe MJ, Dzemidzic M, Lurito JT, Mathews VP, Phillips MD (2000) Correlations in low-frequency BOLD fluctuations reflect cortico-cortical connections. *Neuroimage* 12:582-587.
- Machulda MM, Ward H, Borowski B, Gunter J, Cha R, O'Brien P, Petersen RC, Boeve BF, Knopman D, Tang-Wai D (2003) Comparison of memory fMRI response among normal, MCI, and Alzheimer's patients. *Neurology* 61:500-506.
- Maldjian JA, Laurienti PJ, Kraft RA (2003) An automated method for neuroanatomic and cytoarchitectonic atlas-based interrogation of fMRI data sets. *Neuroimage* 19:1233-1239.
- Marussich L, Lu KH, Wen H (2016) Mapping white-matter functional organization at rest and during naturalistic visual perception. *Neuroimage* 146:1128.
- Mori S, Oishi K, Jiang H (2008) Stereotaxic white matter atlas based on diffusion tensor imaging in an ICBM template. *Neuroimage* 40:570-582.
- Naggara O, Oppenheim C, Rieu D, Raoux N, Rodrigo S, Dalla Barba G, Meder JF (2006) Diffusion tensor imaging in early Alzheimer's disease. *Psychiatry Res* 146:243-249.
- Nanotechnology-based drug delivery systems for Alzheimer's disease management (2017) Technical, industrial, and clinical challenges. *J Control Release* 245:95-107.
- Nestor PJ, Scheltens P, Hodges JR (2004) Advances in the early detection of Alzheimer's disease. *Nat Med* 10:S34.
- Ogawa S, Lee TM, Nayak AS, Glynn P (1990) Oxygenation-sensitive contrast in magnetic resonance image of rodent brain at high magnetic fields. *Magn Reson Med* 14:68-78.
- Qi Z, Wu X, Wang Z, Zhang N, Dong H, Yao L, Li K (2010) Impairment and compensation coexist in amnesic MCI default mode network. *Neuroimage* 50:48-55.
- Quevenco FC, Preti MG, Van Bergen JM, Hua J, Wyss M, Li X, Schreiner SJ, Steininger SC, Meyer R, Meier IB (2017) Memory performance-related dynamic brain connectivity indicates pathological burden and genetic risk for Alzheimer's disease. *Alzheimers Res Ther* 9:24.
- Rombouts SA, Barkhof F, Veltman DJ, Machielsen WC, Witter MP, Bierlaagh MA, Lazeron RH, Valk J, Scheltens P (2000) Functional MR imaging in Alzheimer's disease during memory encoding. *Am J Neuroradiol* 21:1869-1875.
- Rosazza C, Minati L (2011) Resting-state brain networks: literature review and clinical applications. *Neurol Sci* 32:773-785.
- Schmidt SA, Akrofi K, Carpenter-Thompson JR, Husain FT (2013) Default mode, dorsal attention and auditory resting state networks exhibit differential functional connectivity in tinnitus and hearing loss. *PLoS One* 8:e76488.
- Smitha K, Akhil Raja K, Arun K, Rajesh P, Thomas B, Kapilamoorthy T, Kesavadas C (2017) Resting state fMRI: a review on methods in resting state connectivity analysis and resting state networks. *Neuroradiol J* 30:305-317.
- Song CG, Zhang YZ, Wu HN, Cao XL, Guo CJ, Li YQ, Zheng MH, Han H (2018) Stem cells: a promising candidate to treat neurological disorders. *Neural Regen Res* 13:1294-1304.
- Stam C, Jones B, Manshanden I, Van Walsum AvC, Montez T, Verbunt JB, de Munck JC, Van Dijk B, Berendse H, Scheltens P (2006) Magnetoencephalographic evaluation of resting-state functional connectivity in Alzheimer's disease. *Neuroimage* 32:1335-1344.
- Vahdat S, Darainy M, Milner TE, Ostry DJ (2011) Functionally specific changes in resting-state sensorimotor networks after motor learning. *J Neurosci* 31:16907-16915.
- Wang K, Liang M, Wang L, Tian L, Zhang X, Li K, Jiang T (2007) Altered functional connectivity in early Alzheimer's disease: a resting-state fMRI study. *Human Brain Mapp* 28:967-978.
- Wu L, Rosa-Neto P, Hsiung GY, Sadovnick AD, Masellis M, Black SE, Jia J, Gauthier S (2012) Early-onset familial Alzheimer's disease (EO-FAD). *Can J Neurol Sci* 39:436-445.
- Xu J, Wang J, Wimo A, Fratiglioni L, Qui C (2017) The economic burden of dementia in China, 1990-2030: implications for health policy. *Bull World Health Organ* 95:18-26.
- Yetkin FZ, Rosenberg RN, Weiner MF, Purdy PD, Cullum CM (2006) FMRI of working memory in patients with mild cognitive impairment and probable Alzheimer's disease. *Eur Radiol* 16:193-206.
- Zhang L, Liu JJ, Zhao Y, Liu Y, Lin JW (2019) N-butylphthalide affects cognitive function of APP/PS1 transgenic mice (Alzheimer's disease model). *Zhongguo Zuzhi Gongcheng Yanjiu* 23:3025-3030.
- Zhao H (2016) Embryonic neural stem cell transplantation for Alzheimer's disease. *Zhongguo Zuzhi Gongcheng Yanjiu* 20:4805-4810.
- Zhou B, Liu Y, Zhang Z, An N, Yao H, Wang P, Wang L, Zhang X, Jiang T (2013) Impaired functional connectivity of the thalamus in Alzheimer's disease and mild cognitive impairment: a resting-state fMRI study. *Curr Alzheimer Res* 10:754-766.

P-Reviewers: Fernandez-Vega I, Dimitriadis SI; C-Editor: Zhao M; S-Editors: Wang J, Li CH; L-Editors: Wright A, Maxwell R, Qiu Y, Song LP; T-Editor: Jia Y